High-Energy Astroparticle Theory

A.Y. 2025/26

Carmelo Evoli

Last updated: November 26, 2025

This document is currently under active development. The content is subject to change as revisions are ongoing. I expect to release a stable and comprehensive version no earlier than November 2026.

These lecture notes are largely based on:

- P. Blasi, *The origin of galactic cosmic rays*, A&AR, 21, 70, 2013, arXiv:1311.7346
- P.D. Serpico, *Cosmic ray interactions with matter and radiation*, Proceedings of the International School of Physics "Enrico Fermi", Course 208, Varenna 2022, arXiv:2308.04361
- D. Boncioli, *Cosmic-ray propagation in extragalactic space and secondary messengers*, Proceedings of the International School of Physics "Enrico Fermi", Course 208, Varenna 2022, arXiv:2309.12743
- C. Evoli & U. Dupletsa, *Phenomenological models of Cosmic Ray transport in Galaxies*, Proceedings of the International School of Physics "Enrico Fermi", Course 208, Varenna 2022, arXiv:2309.00298

Useful readings:

- M. Vietri, *Foundations of High-Energy Astrophysics*, April 2008, U. Chicago Press
- R. Blandford & D. Eichler, *Particle acceleration at astrophysical shocks: A theory of cosmic ray origin*, October 1987, Physics Reports, 154
- G.B. Rybicki & A.P. Lightman, *Radiative Processes in Astrophysics*, May 1985, Vch Pub
- T.K. Gaisser, R. Engel & E. Resconi, *Cosmic Rays and Particle Physics*, June 2016, Cambridge University Press
- D. Overbye, *Lonely Hearts of the Cosmos: The Story of the Scientific Quest for the Secret of the Universe*, November 1999, Back Bay Books

Contents

1 Radiative Processes in Astroparticle Physics

1.1 The Multi-Messenger View of Astroparticle Physics

Astroparticle physics is inherently *multi-messenger*: we learn about high-energy processes in the Universe by combining information from charged cosmic rays (CRs), photons across the electromagnetic spectrum (from radio to TeV–PeV γ-rays), neutrinos, and—when relevant—gravitational waves. Each messenger samples different interactions and environmental scales; together they allow us to disentangle acceleration, transport, and radiation in complex sources and along their lines of sight.

Why radiative processes matter. Radiative processes both *encode* conditions in the source/medium and *reshape* the underlying particle populations. Interactions of energetic particles with magnetic and radiation fields or with matter—most notably synchrotron, bremsstrahlung, inverse Compton (IC), and hadronic interactions leading to pion production—cause energy losses that can be competitive with acceleration and escape. These losses modify particle spectra (cooling breaks, cutoffs), and therefore the photon and neutrino spectra we observe. For leptons, synchrotron and IC cooling often dominate; for hadrons, inelastic pp and photo-hadronic processes are usually sub-dominant in the diffuse interstellar medium (ISM) but can be decisive in dense or radiation-rich environments (e.g., starbursts, AGN cores).

Secondary emission as a diagnostic. Even when a particular channel is energetically sub-dominant for transport, its byproducts can be exceptionally informative. A prime example is the diffuse Galactic γ-ray emission: photons from π^0 decay (produced in CR proton–gas collisions), plus bremsstrahlung and IC from CR electrons, map the spatial distribution of CR densities, gas, and interstellar radiation fields. In the Milky Way's ISM, pion production contributes little to the *transport* of CR protons (loss times exceed significantly escape at GeV–TeV energies), yet the resulting γ-rays are one of our cleanest tracers of hadronic CRs on kiloparsec scales. Analogously, high-energy neutrinos directly tag hadronic interactions in environments opaque to γ-rays.

In conclusion, multi-messenger observations transform radiative byproducts into diagnostics of acceleration sites and propagation. The same processes that light up the sky

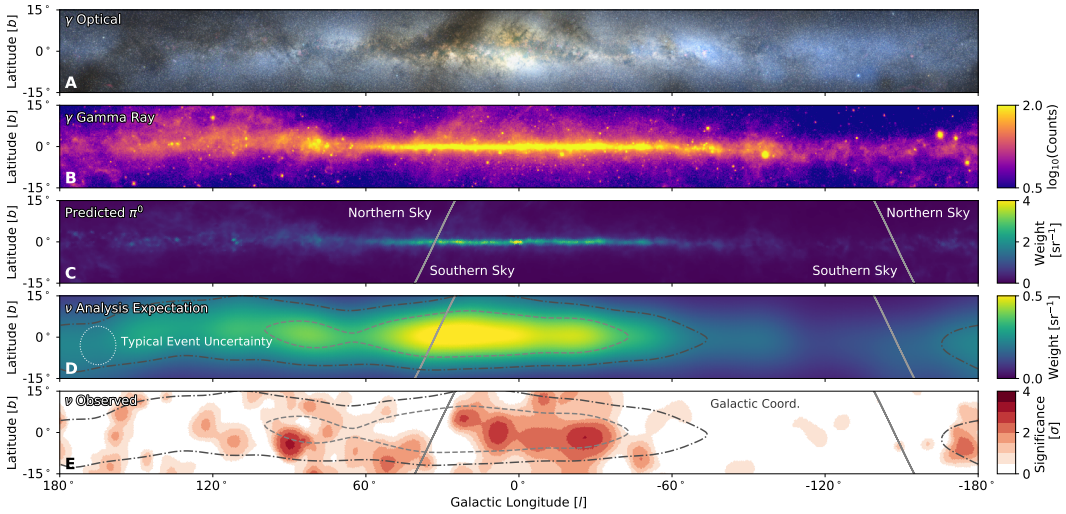

Figure 1.1: The Milky Way in photons and neutrinos. All panels are Galactic coordinates (±15° in latitude, ±180° in longitude). (A) Optical image—partly obscured by dust (credit: A. Mellinger) [?]. (B) Fermi-LAT diffuse γ-ray flux integrated over 1 GeV (12-year map) [?]. (C) Expected neutrino template from a π^0 model matched to the Fermi-LAT diffuse emission. (D) Template folded with IceCube cascade response. (E) IceCube pre-trial significance from an all-sky cascade search; contours overlay the hadronic template predicted from γ rays as in (D). Spatial overlap with hot spots is suggestive, but not conclusive without a robust post-trial significance.

also modify the parent particle distributions. A careful accounting of energy loss, target fields, and escape is therefore the backbone of any high-energy astroparticle inference.

[ADD HERE THE COSMIC RAY PLOT.]

1.2 Kinetic equation for particles with radiative losses

We begin with a minimal model to show how continuous energy losses lead to a kinetic (continuity) equation for the particle distribution, such that the steady state differs from the injected spectrum, producing observable spectral imprints that diagnose regions of particle acceleration.

[CITE LONGAIR HERE]

Let $N(E,t)$ be the differential ***number density*** per unit energy ($\mathrm{L}^{-3}\,\mathrm{E}^{-1}$), and $Q(E,t)$ the ***injection rate density*** ($\mathrm{L}^{-3}\,\mathrm{T}^{-1}\,\mathrm{E}^{-1}$). Energy losses are

$$\dot{E} \equiv \frac{dE}{dt} = -\,b(E), \qquad b(E) > 0,$$

and optional escape is parameterized by a residence time $\tau_{\rm esc}(E)$.

Consider the bin $[E, E+\Delta E]$ at time t. The particles in this bin came, a short time Δt earlier, from $[E', E'+\Delta E']$ with the backward map

$$E' = E + b(E)\,\Delta t, \qquad E' + \Delta E' = (E+\Delta E) + b(E+\Delta E)\,\Delta t. \tag{1.1}$$

Band	Wavelength λ [m]	Frequency ν [Hz]	Energy E [eV]
Radio	$\sim 1 - 10^{4}$	$\sim 10^{4} - 3\times10^{8}$	$\sim 4\times10^{-11} - 10^{-6}$
Microwaves	$\sim 10^{-3} - 1$	$\sim 3\times10^{8} - 3\times10^{11}$	$\sim 10^{-6} - 10^{-3}$
Infrared (IR)	$\sim 10^{-6} - 10^{-3}$	$\sim 3\times10^{11} - 4\times10^{14}$	$\sim 10^{-3} - 2$
Visible (optical)	$\sim 4\times10^{-7} - 7\times10^{-7}$	$\sim 4\times10^{14} - 7.5\times10^{14}$	$\sim 1.6 - 3$
Ultraviolet (UV)	$\sim 10^{-8} - 4\times10^{-7}$	$\sim 7.5\times10^{14} - 3\times10^{16}$	$\sim 3 - 10^{2}$
X-rays	$\sim 10^{-11} - 10^{-8}$	$\sim 3\times10^{16} - 3\times10^{19}$	$\sim 10^{2} - 10^{5}$
Gamma rays	$\lesssim 10^{-11}$	$\gtrsim 3\times10^{19}$	$\gtrsim 10^{5}$

Table 1.1: Approximate ranges of the electromagnetic spectrum in wavelength, frequency, and photon energy. Boundaries between bands are conventional and may vary slightly between sources.

A first–order Taylor expansion in ΔE gives the Jacobian factor

$$\Delta E' = \Delta E + \frac{\partial b}{\partial E}\,\Delta E\,\Delta t. \tag{1.2}$$

Number conservation between t and $t + \Delta t$ implies

$$N(E, t + \Delta t)\,\Delta E = N(E', t)\,\Delta E'. \tag{1.3}$$

Expand to first order in Δt:

$$N(E, t + \Delta t) = N(E, t) + \frac{\partial N}{\partial t}\,\Delta t, \qquad N(E', t) = N(E, t) + \frac{\partial N}{\partial E}\,b(E)\,\Delta t. \tag{1.4}$$

Insert (1.4) into (1.3), keep only $O(\Delta t)$, and cancel the common $N\,\Delta E$:

$$\frac{\partial N}{\partial t}\,\Delta t\,\Delta E = \frac{\partial N}{\partial E}\,b\,\Delta t\,\Delta E + N\,\frac{\partial b}{\partial E}\,\Delta t\,\Delta E. \tag{1.5}$$

Divide by $\Delta t\,\Delta E$ and take $\Delta t \to 0$:

$$\frac{\partial N}{\partial t} = \frac{\partial}{\partial E}[b(E)\,N(E, t)]\,. \tag{1.6}$$

This is the continuity equation in energy space (with no sources/sink yet): the term $\partial_E[bN]$ is the energy–space flux that ***advects*** particles from high to low energy. The origin of the $\partial_E b$ piece is the Jacobian $\Delta E'/\Delta E = 1 + (\partial_E b)\Delta t$.

Injection adds $Q(E, t)\,\Delta E\,\Delta t$ particles to the bin, while escape removes $\left[N(E, t)\tau_{\rm esc}^{-1}(E)\right]\Delta E\,\Delta t$. Repeating the same first–order expansion yields the full kinetic (continuity) equation

$$\frac{\partial N}{\partial t} = \frac{\partial}{\partial E}[b(E)\,N(E, t)] \;-\; \frac{N(E, t)}{\tau_{\rm esc}(E)} \;+\; Q(E, t)\,. \tag{1.7}$$

This equation describes how a particle distribution, sourced by Q, evolves under radiative losses and escape. One can obtain (1.7) equivalently by angle– and volume–integrating the phase–space Vlasov equation and projecting onto energy; the bin–mapping derivation above is however the most transparent for a first exposure.

Equilibrium spectrum with radiative losses. In steady state ($\partial_t N = 0$) the kinetic equation (1.7) solves to

$$N(E) = \frac{1}{b(E)} \int_E^\infty Q(E')\, dE' \,, \tag{1.8}$$

if escape is neglected, i.e. $\tau_{\rm esc} \to \infty$, and

$$N(E) = \frac{1}{\mu(E)} \int_E^\infty \frac{\mu(E')\, Q(E')}{b(E')}\, dE', \quad \mu(E) \equiv \exp\left[\int^E \frac{dE''}{b(E'')\, \tau_{\rm esc}(E'')}\right] \,, \tag{1.9}$$

if escape is competitive with losses.

Monochromatic injection For continuous, ***monoenergetic injection*** $Q(E) = Q_0\, \delta(E - E_{\rm inj})$ and no escape, equation (1.8) gives

$$N(E) = \frac{Q_0}{b(E)} \,, \quad \text{for } E < E_{\rm inj} \,. \tag{1.10}$$

Thus the steady spectrum below $E_{\rm inj}$ mirrors the loss law: if $b(E) \propto E^m$, with $m > 0$, then

$$N(E) \propto E^{-m} \,, \quad \text{for } E < E_{\rm inj} \,.$$

Spectral steepening. For a ***power–law injection*** $Q(E) = Q_0 E^{-p}$ ($p > 1$) and losses $b(E) = b_0 E^m$ ($m > 0$), equation (1.8) gives

$$N(E) \propto \frac{E^{-(p-1)}}{E^m} = E^{-(p+m-1)}. \tag{1.11}$$

Thereby radiative cooling steepens the index by $m - 1$ relative to the injection index p. For synchrotron/IC in the Thomson regime (see section X) $m = 2$: an injected spectrum with $p = 2$ yields an equilibrium spectrum $N \propto E^{-3}$ in the cooling–dominated range.

The cooling break. If particles are continuously injected for a time t_* ***without*** radiative losses, the spectrum simply accumulates:

$$N(E) \;\simeq\; Q(E)\, t_{\rm res}(E), \qquad t_{\rm res}(E) = \min\left[t_*,\, \tau_{\rm esc}(E)\right]. \tag{1.12}$$

This "reservoir'' picture shows that when $t_* \ll \tau_{\rm esc}(E)$ the equilibrium spectrum follows the injected slope: $N(E) \approx Q(E)\, t_*$.

Radiative losses introduce an energy–dependent residence time. When cooling is the fastest process, particles are advected through energy too quickly to accumulate, and the steady state is no longer $Q \times t_*$ but instead from equation (1.11) we derive

$$N(E) \;=\; \frac{1}{b(E)} \int_E^\infty Q(E')\, dE' \;\approx\; Q(E)\, \frac{E}{b(E)} \;=\; Q(E)\, t_{\rm cool}(E), \tag{1.13}$$

where $t_{\rm cool}(E) \equiv E/b(E)$ and the approximation holds for smooth Q.

The transition between the two regimes occurs at the ***cooling break***[1] $E_{\rm c}$ defined by

$$t_{\rm cool}(E_{\rm c}) \;\simeq\; \min[t_*,\, \tau_{\rm esc}(E_{\rm c})]\,.$$

For power-law losses $b(E) = b_0 E^m$ with $m > 1$, and age-limited cooling:

$$E_{\rm c} \;\simeq\; \left[\frac{1}{(m-1)\, b_0\, t_*}\right]^{1/(m-1)}, \quad (m = 2:\; E_{\rm c} \simeq 1/(b_0 t_*)). \tag{1.14}$$

Assuming a power-law injection $Q(E) \propto E^{-p}$, we then have the canonical broken behavior:

$$N(E) \propto \begin{cases} E^{-p}, & E \ll E_{\rm c} \quad \text{(no significant cooling; age/escape limited)}, \\ E^{-(p+m-1)}, & E \gg E_{\rm c} \quad \text{(cooling dominated)}. \end{cases}$$

Thus the spectral index steepens by $\Delta\alpha = m - 1$ across the break; in particular, for synchrotron/IC in the Thomson regime ($m = 2$) the steepening is +1. Locating $E_{\rm c}$ is therefore highly diagnostic: it ties together the source age (or escape time) and the strength of the target fields that set $b(E)$.

[Add exercise for Crab.]

Injection burst and cooling cutoff. For a burst at $t = 0$, radiative losses *advect* particles through energy. The characteristic relation is

$$\int_{E(t)}^{E_i} \frac{dE'}{b(E')} = t, \qquad \text{with} \quad \dot{E} = -b(E). \tag{1.15}$$

For power-law losses $b(E) = b_0 E^m$ with $m > 1$,

$$E_i(E, t) \;=\; \left[E^{\,1-m} + (1-m)\, b_0\, t\right]^{1/(1-m)}. \tag{1.16}$$

This inversion only exists if the bracket is positive. For $m > 1$ this implies

$$E^{1-m} > (m-1)\, b_0\, t \quad \rightarrow \quad E < E_{\rm cut}(t)\,, \tag{1.17}$$

[1] The term "cooling break" is in common use but potentially misleading: the particles are non-thermal and no well-defined temperature exists for the power-law population. What we call "cooling" is really phase-space *advection in energy* due to continuous radiative losses, not thermodynamic cooling of a Maxwellian gas. A more precise term would be "radiative-loss break'' (or simply "loss break''). We keep the conventional nomenclature for continuity with the literature.

with the ***cooling cutoff***:

$$E_{\rm cut}(t) = [(m-1)\, b_0\, t]^{-1/(m-1)}\,, \qquad (m=2:\ E_{\rm cut} = 1/(b_0 t))\,. \tag{1.18}$$

Physically, the spectrum is emptied above $E_{\rm cut}(t)$ because, for super-linear losses, particles traverse those energies in a *finite* time. Once the elapsed time exceeds the passage time to cool from ∞ down to E, no initial energy E_i exists that could have cooled to E by time t ($\rightarrow$ the inversion $E_i(E,t)$ has no solution), hence $N(E,t) = 0$ for $E \geq E_{\rm cut}(t)$. Under ***continuous*** injection, this sharp cutoff is replaced by a ***cooling break***; for a ***single burst*** it remains a time-dependent high-energy cutoff at $E_{\rm cut}(t)$.

[say more about cooling spike]

1.3 Synchrotron Radiation

Synchrotron radiation, schematically $e + B \rightarrow e + \gamma + B$, is emitted when a *relativistic* charged particle is accelerated in the presence of a magnetic field. In the non-relativistic limit this is known as *cyclotron emission*.

In c.g.s. units, the non-relativistic Larmor power radiated by a charge q with acceleration magnitude $a = \|\mathbf{a}\|$ is

$$P_{\rm Larmor} = \frac{2}{3}\frac{q^2 a^2}{c^3}\,. \tag{1.19}$$

Notice that radiative effects scale as q^2, since cross sections go like the square of the amplitude and e.m. amplitudes are $\propto q$.

Relativistically, the correct generalization is the *Liénard* formula,

$$P = \frac{2}{3}\frac{q^2\gamma^6}{c^3}\Big(a^2 - (\boldsymbol{\beta}\times\mathbf{a})^2\Big) = \frac{2}{3}\frac{q^2\gamma^4}{c^3}\Big(a_\perp^2 + \gamma^2 a_\parallel^2\Big), \tag{1.20}$$

where $\boldsymbol{\beta} = \mathbf{v}/c$, and $a_\perp$ and $a_\parallel$ are the components of $\mathbf{a}$ perpendicular and parallel to $\mathbf{v}$, respectively.

[add the full derivation from the covariant expression of Larmor?]

Motion in a magnetic field and synchrotron power for a single charge. For a purely magnetic field the Lorentz force does no work and the acceleration is perpendicular to $\mathbf{v}$ (appendix A.1). Using $\dot{\mathbf{p}} = q\,\mathbf{v}\times\mathbf{B}/c$ with $\mathbf{p} = \gamma m \mathbf{v}$, the *perpendicular* acceleration is

$$a_\perp = \frac{q\, v_\perp\, B}{\gamma\, m\, c} = \frac{q\, B}{\gamma\, m\, c}\, v \sin\theta, \tag{1.21}$$

where θ is the pitch angle. Substituting $a_\parallel = 0$ and this $a_\perp$ into (1.20) gives the radiated power of a single relativistic particle:

$$P_{\rm s} = \frac{2}{3}\frac{q^4 B^2}{m^2 c^3}\,\gamma^2\,\beta^2\,\sin^2\theta \xrightarrow{\beta\rightarrow 1} \frac{2}{3}\frac{q^4 B^2}{m^2 c^3}\,\gamma^2\,\sin^2\theta. \tag{1.22}$$

For an isotropic distribution of pitch angles,

$$\langle \sin^2\theta \rangle = \frac{1}{4\pi}\int d\Omega\, \sin^2\theta = \frac{2}{3}.$$

Averaging (1.22) and using $U_B = B^2/(8\pi)$ and $\sigma_T = \frac{8\pi}{3}\left(\frac{q^2}{m_e c^2}\right)^2$ yields the familiar compact form

$$\langle P_s \rangle = \frac{4}{9}\frac{q^4 B^2}{m^2 c^3}\gamma^2 = \frac{4}{3}\, c\, \sigma_T \left(\frac{m_e}{m}\right)^2 \gamma^2\, U_B \ . \tag{1.23}$$

Notice that at ***fixed particle energy*** $E = \gamma m c^2$, one has $\gamma \propto 1/m$, hence $P_s \propto \gamma^2/m^2 \propto m^{-4}$. This steep mass dependence makes synchrotron losses overwhelmingly important for electrons and positrons compared to nuclei. Moreover, it is important to remark that the energy loss is ***proportional to the magnetic field energy density*** U_B.

Cooling time. For electrons ($m = m_e$) the synchrotron loss time is

$$\tau_{\rm loss}(\gamma) \ = \ \frac{E}{|dE/dt|} = \frac{\gamma m_e c^2}{\langle P_s \rangle} = \frac{3}{4}\frac{m_e c}{\sigma_T}\frac{1}{\gamma\, U_B} \ \propto \ \frac{1}{E}\,. \tag{1.24}$$

Thus ***higher-energy*** electrons cool ***faster***, a key driver of spectral steepening in synchrotron-dominated sources.

Numerically, we can estimate for electrons

$$\tau_{\rm loss}(E_e) \simeq 0.3\ {\rm Myr}\left(\frac{U_B}{\rm eV\ cm^{-3}}\right)^{-1}\left(\frac{E}{\rm TeV}\right)^{-1} \tag{1.25}$$

From beaming to the single-electron spectrum. To obtain the spectrum of a single electron at fixed energy, we view P_ν as the Fourier transform of the time-domain power $P(t)$, which in turn tracks $|\mathbf{a}(t)|^2$. Relativistic beaming is the key ingredient: the emission is confined within a cone of half-angle $\sim 1/\gamma$ centered on $\mathbf{v}$. As the electron gyrates, an observer sees short pulses whenever the beam sweeps across the line of sight; the Fourier transform of these pulses yields a broad spectrum extending to frequencies $\gg$ the gyrofrequency.

Relativistic aberration. Assume the primed frame moves with speed βc along x relative to the unprimed (observer) frame. Lorentz transforms:

$$ct' = \gamma(ct - \beta x), \quad x' = \gamma(x - \beta ct), \quad y' = y\,.$$

Velocity components transform as

$$u_x = \frac{u'_x + \beta c}{1 + \beta u'_x/c}, \qquad u_y = \frac{u'_y}{\gamma\left(1 + \beta u'_x/c\right)}.$$

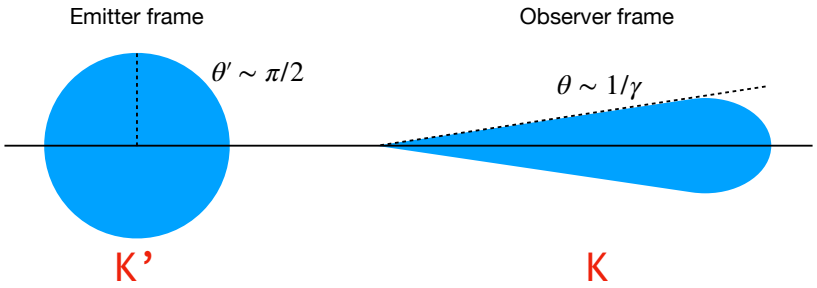

Figure 1.2: An isotropic pattern in the emitter frame is concentrated into a narrow cone $\sim 1/\gamma$ about the velocity in the observer frame.

Hence the emission angle θ satisfies

$$\tan\theta = \frac{u_y}{u_x} = \frac{u'_y}{\gamma(u'_x + \beta c)} = \frac{u' \sin\theta'}{\gamma(\beta c + u' \cos\theta')}.$$

For light ($u' = c$) one obtains the standard ***aberration formula***:

$$\tan\theta = \frac{\sin\theta'}{\gamma\left(\beta + \cos\theta'\right)}. \tag{1.26}$$

A photon emitted at $\theta' = 0$ is seen at $\theta = 0$, while a photon emitted at $\theta' = \pi/2$ is seen at $\theta \simeq 1/\gamma$ for $\gamma \gg 1$. Thus emission that is isotropic in the emitter frame becomes forward-beamed in the observer frame—a fact central to synchrotron pulses and to strongly beamed phenomena such as GRB jets.

Pulse duration and characteristic frequency. In the non-relativistic limit the emission is essentially mono-chromatic at the gyrofrequency ν_0, because the charge executes uniform circular motion and the radiation pattern is broad.

[add a plot with a(t) and frequency]

For relativistic particles, beaming squeezes the emission into a cone of half–opening $\sim 1/\gamma$ about the instantaneous velocity. An observer only "sees" the electron while this cone sweeps across the line of sight, so the continuous emission is received as a train of short pulses. The spectrum we measure is the Fourier transform of this time-domain signal, and it is therefore controlled by the *observed* pulse width $\Delta t_{\rm obs}$: the characteristic frequency scales like $\nu_{\rm s} \sim 1/\Delta t_{\rm obs}$.

Let the line of sight be nearly aligned with the velocity at the time the beam points toward the observer (see Fig. 1.3). The visibility condition $|\Delta\phi| \lesssim 1/\gamma$ translates into a small orbital phase window

$$\Delta\phi \sim \frac{2}{\gamma}.$$

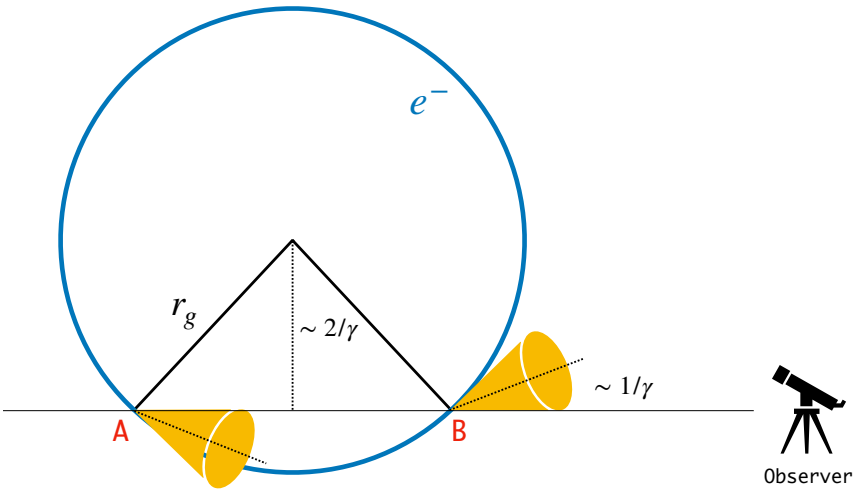

Figure 1.3: As the electron gyrates, its emission is confined to a cone of half–opening $\sim 1/\gamma$ about the instantaneous velocity. The observer only receives radiation while the cone sweeps across the line of sight (between points A and B), a phase interval $\Delta\phi \sim 2/\gamma$.

The *emission* duration in the lab frame is then

$$\Delta t \;\sim\; \frac{\Delta\phi}{\Omega_B} \;=\; \frac{2/\gamma}{\Omega_0/\gamma} \;=\; \frac{2}{\Omega_0}\,,$$

using $\Omega_B = \Omega_0/\gamma$ with $\Omega_0 \equiv qB/(mc)$.

Because later photons start closer to the observer, their travel times are shorter (δt_i is the time for the *photon* to reach the observer):

$$\Delta t_{\rm obs} = t_B + \delta t_B - (t_A + \delta t_A) = (t_B - t_A) + (\delta t_B - \delta t_A) = \frac{\rm AB}{v} - \frac{\rm AB}{c} = \Delta t(1-\beta)\,, \quad (1.27)$$

this compresses the received pulse by roughly a factor $2\gamma^2$:

$$\Delta t_{\rm obs} \;=\; \Delta t\,(1-\beta) \;\simeq\; \frac{\Delta t}{2\gamma^2} \;\;\Rightarrow\;\; \Delta t_{\rm obs} \;\sim\; \frac{1}{\gamma^2\,\Omega_0}\,. \quad (1.28)$$

Equivalently, using $r_g = v_\perp/\Omega_B$,

$$\Delta t_{\rm obs} \;\sim\; \frac{r_g}{\gamma^3\, v_\perp}\,, \quad (1.29)$$

so an ultra-relativistic electron ($v_\perp \simeq c$) produces narrow pulses whose width shrinks like γ^{-3} at fixed r_g.

The observer therefore measures a broadband spectrum peaked at

$$\nu_{\rm s} \sim \frac{1}{\Delta t_{\rm obs}} \;\sim\; \gamma^2\,\nu_0\,, \quad (1.30)$$

i.e. boosted by γ^2 relative to the cyclotron frequency ν_0. The pulses recur every gyroperiod $T = 2\pi/\Omega_B = \gamma/\nu_0$.

Single–electron spectrum (full calculation). A rigorous way to derive the synchrotron spectrum is to treat the motion *locally* as curvature radiation: over the short visibility arc the trajectory is well approximated by a circle of curvature radius $\rho = r_g/\sin\theta$ (only the perpendicular acceleration radiates). This fixes the *characteristic* or *critical* frequency at which most power is concentrated,

$$\nu_c = \frac{\omega_c}{2\pi} = \frac{3}{2}\,\gamma^2\,\nu_0\,\sin\theta = \frac{3}{4\pi}\,\frac{qB}{mc}\,\gamma^2\sin\theta. \tag{1.31}$$

Numerically, the critical frequency for a GeV electron in a typical ISM field is in the *radio waves*:

$$\nu_c \simeq 16\ \mathrm{Mhz}\,\left(\frac{E}{\mathrm{GeV}}\right)^2\left(\frac{B}{\mu\mathrm{G}}\right) \tag{1.32}$$

The remarkable fact—derived by a full Fourier analysis of the Liénard–Wiechert fields—is that the entire single–electron spectrum takes a compact, universal form:

$$P_\nu(\nu,\gamma,\theta) = \frac{\sqrt{3}\,q^3B}{m_e c^2}\,\sin\theta\,F\!\left(\frac{\nu}{\nu_c}\right), \qquad F(x) = x\int_x^\infty K_{5/3}(x')\,dx'. \tag{1.33}$$

Here F is the *synchrotron kernel* (built from the modified Bessel function $K_{5/3}$), which encodes the spectral *shape*, while the prefactor sets the *amplitude* via B and the radiating component of the acceleration ($\propto \sin\theta$). Two asymptotic limits reproduce the canonical look of synchrotron spectra,

$$F(x) \simeq \begin{cases} 2.15\,x^{1/3}, & x \equiv \nu/\nu_c \ll 1, \\ \sqrt{\dfrac{\pi x}{2}}\,e^{-x}, & x \gg 1, \end{cases}$$

yielding the familiar low–frequency behaviour $P_\nu \propto \nu^{1/3}$ and an exponential suppression above ν_c. Between these regimes the energy–weighted curve νP_ν attains a well–defined maximum at $\nu_{\max} \simeq 0.29\,\nu_c$ (see Fig. 1.4); in practice, one often plots spectra against ν/ν_c and reads the shape off once and for all.

As useful checks:

- integrating P_ν over ν returns the Larmor/Liénard total power (and, after pitch–angle averaging, the standard factor $\langle\sin^2\theta\rangle = 2/3$), confirming the kernel's normalization;
- for back-of-the-envelope estimates, the ***delta approximation*** collapses the spectrum to $P_\nu \simeq P_s\,\delta(\nu-\nu_c)$ and reproduces the correct scalings with B, γ, and θ;
- the explicit $\sin\theta$ reminds us that synchrotron is powered by the ***perpendicular*** acceleration: no pitch angle, no radiation.

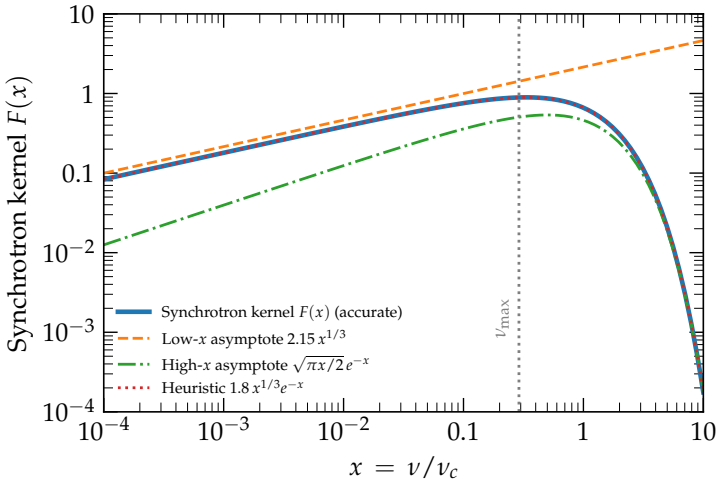

Figure 1.4: The synchrotron kernel $F(x)$ describing the synchrotron spectrum emitted by the single electron. Exact $F(x) = x\int_x^\infty K_{5/3}$ (solid) with low-/high-x asymptotes and the heuristic $1.8\,x^{1/3}e^{-x}$.

1.4 Synchrotron emission by an electron population.

In most sources the radiating electrons span a broad range of energies. The most common modelization of the parent electron population is a power–law in Lorentz factor,

$$n(\gamma)\,d\gamma = n_0\,\gamma^{-p}\,d\gamma, \qquad \gamma_{\rm min} < \gamma < \gamma_{\rm max},$$

where n is the differential number density (L^{-3}) and the typical slopes in many astrophysical environments ranges in $p \simeq 2$–3 . The specific emissivity (power per unit volume and frequency) follows by summing the single–electron spectra over the population and pitch angles,

$$j_\nu \;=\; \int_{\gamma_{\rm min}}^{\gamma_{\rm max}} \langle P_\nu(\gamma,\theta)\rangle\, n(\gamma)\,d\gamma,$$

where $\langle\cdots\rangle$ denotes an average over pitch angle (isotropic unless stated).

To expose the scalings, we approximate each spectrum by a delta-function at its critical frequency,

$$P_\nu(\gamma,\theta) \;\simeq\; \langle P_{\rm s}(\gamma)\rangle\;\delta\big(\nu-\nu_c(\gamma,\theta)\big),$$

with $\langle P_{\rm s}(\gamma)\rangle$ as in 1.23, and $\nu_c(\gamma,\theta)$ as in 1.31.

Inserting the δ–function, and using the identity

$$\delta\big(\nu-\nu_c(\gamma)\big) = \frac{\delta\big(\gamma-\gamma_\nu\big)}{\left|\frac{d\nu_c}{d\gamma}\right|_{\gamma_\nu}}, \qquad \gamma_\nu \;\equiv\; \sqrt{\frac{\nu}{\frac{3}{2}\nu_0\sin\theta}}, \tag{1.34}$$

we obtain

$$j_\nu = \int_{\gamma_{\rm min}}^{\gamma_{\rm max}} n_0\,\gamma^{-p}\,\langle P_{\rm s}(\gamma)\rangle\,\delta\big(\nu-\nu_c(\gamma)\big)\,d\gamma = n_0\,\frac{\frac{4}{3}c\sigma_{\rm T}U_B\,\gamma_\nu^{2-p}}{2\,(\frac{3}{2}\nu_0\sin\theta)\,\gamma_\nu} \propto B^{\frac{p+1}{2}}\,\nu^{-\frac{p-1}{2}}\,. \tag{1.35}$$

	Source: monochromatic $Q(E) = Q_0\,\delta(E - E_0)$	**Source: power-law** $Q(E) = Q_0\,E^{-p}$
Equilibrium electron spectrum	$N(E) \propto E^{-2}$	$N(E) \propto E^{-(p+1)}$
Synchrotron spectrum	$j_\nu \propto \nu^{-1/2}$	$j_\nu \propto \nu^{-p/2}$

Table 1.2: Electron and synchrotron slopes for cooling–dominated steady state (assuming no escape).

Thus we recover the ***synchrotron law***:

$$j_\nu \;\propto\; n_0\, B^{\frac{p+1}{2}}\, \nu^{-\frac{p-1}{2}} \quad \text{for} \quad \nu_{\min} < \nu < \nu_{\max}, \tag{1.36}$$

where the validity band is set by the lowest and highest electrons that can radiate at ν,

$$\nu_{\min} \equiv \nu_c(\gamma_{\min}) \simeq \frac{3}{2}\,\gamma_{\min}^2\,\nu_0\,\langle \sin\theta \rangle, \qquad \nu_{\max} \equiv \nu_c(\gamma_{\max}). \tag{1.37}$$

Below the band, the low–frequency tail of the single–electron kernel dominates:

$$j_\nu \;\propto\; \nu^{1/3} \qquad (\nu \ll \nu_{\min}).$$

Above the band, the high–frequency tail is exponentially suppressed by the kernel of the *highest* electrons present:

$$j_\nu \;\propto\; \exp\!\left(-\frac{\nu}{\nu_{\max}}\right) \qquad (\nu \gg \nu_{\max}).$$

In conclusion, an electron index p produces a synchrotron index

$$\alpha \equiv -\frac{d\ln j_\nu}{d\ln \nu} = \frac{p-1}{2}.$$

The amplitude scales as $B^{(p+1)/2}$, not B^2, because the characteristic frequency of each electron also shifts with B. Replacing the δ-function with the full kernel leaves the ν– and B–scalings unchanged and only multiplies j_ν by a smooth function of p.

[Add example for Galaxy synchrotron spectrum: frequency vs energy / slope]

[say something about polarization]

1.5 Inverse Compton Scattering

Inverse Compton (IC) scattering is, in many ways, the *radiative sibling* of synchrotron emission. In both cases, relativistic electrons lose energy by interacting with an ambient

field: for synchrotron, it is the magnetic field; for IC, it is a bath of photons. In the IC process, background photons are *up-scattered* by high-energy electrons,

$$e + \gamma \longrightarrow e' + \gamma'$$

so that low-energy photons (e.g. CMB or starlight) emerge at much higher energies (X-rays, γ rays). Whenever electron energies are much larger than those of the target photons, IC becomes an efficient *energy-loss* mechanism for the electrons and a powerful high-energy radiation channel.

Before moving to the fully relativistic and quantum description, it is instructive to recover the basic scaling of IC power from a classical perspective and to see how the Thomson cross-section naturally appears.

Thomson scattering. In the classical picture, an electromagnetic wave impinges on an electron, forcing it to oscillate and therefore to radiate due to its accelerated motion. The Poynting flux $\mathbf{S}$ of a plane wave incident on the electron is

$$\mathbf{S} = \frac{c}{4\pi}\,\mathbf{E}\times\mathbf{B} \quad\Rightarrow\quad S \equiv |\mathbf{S}| = \frac{c}{4\pi}|\mathbf{E}|^2\,,$$

where in the last step we used $|\mathbf{E}| = |\mathbf{B}|$ for an electromagnetic wave in vacuum.

The Lorentz force acting on the electron is

$$\mathbf{F} = q\left(\mathbf{E} + \frac{\mathbf{v}}{c}\times\mathbf{B}\right) \simeq q\mathbf{E}\,,$$

where we have assumed $|\mathbf{v}| \ll c$, so that the magnetic contribution to the force is negligible compared to the electric one.

We write the oscillating electric field of the wave as

$$\mathbf{E} = E_0\,\epsilon\,\sin\!\big(\omega t + \phi\big)\,,$$

with ϵ a unit polarization vector. The electron acceleration is then

$$\mathbf{a} = \frac{\mathbf{F}}{m} = \frac{q}{m}\mathbf{E}\,,$$

and its time-averaged squared magnitude is

$$\langle a^2\rangle = \left(\frac{q}{m}\right)^2\langle E^2\rangle = \left(\frac{q}{m}\right)^2\frac{E_0^2}{2}\,,$$

where we used

$$\frac{1}{T}\int_0^{T=\frac{2\pi}{\omega}} \sin^2(\omega t)\,dt = \frac{1}{2}\,.$$

The average power radiated by an accelerated charge in the non-relativistic limit is given by the Larmor formula (1.19):

$$\langle P\rangle = \frac{2}{3}\frac{q^2\langle a^2\rangle}{c^3} = \frac{2}{3}\frac{q^2}{c^3}\left(\frac{q^2}{m^2}\frac{E_0^2}{2}\right) = \frac{1}{3}\frac{q^4}{m^2c^3}E_0^2\,.$$

The classical cross-section associated with this scattering process is defined as the ratio between the power radiated by the electron and the incident flux. Using the time-averaged Poynting flux

$$\langle S \rangle = \frac{c}{8\pi} E_0^2 \,,$$

we write

$$\langle P \rangle = \sigma_{\rm T} \langle S \rangle \quad \Rightarrow \quad \sigma_{\rm T} = \frac{\langle P \rangle}{\langle S \rangle} = \frac{1}{3} \frac{q^4}{m^2 c^3} E_0^2 \, \frac{8\pi}{c} \, \frac{1}{E_0^2} = \frac{8}{3} \pi \left(\frac{q^2}{mc^2} \right)^2 .$$

This quantity,

$$\sigma_{\rm T} \simeq 6.652 \times 10^{-25} \ {\rm cm}^2 \,,$$

is the well-known ***Thomson cross-section***. In words: the electron intercepts and re-radiates the power corresponding to the flux crossing an effective area $\sigma_{\rm T}$, redistributing it over the familiar doughnut-shaped pattern given by the Larmor radiation.

Once the Thomson cross-section is known, the time-averaged power scattered by a ***single*** electron in an isotropic radiation field of energy density $U_{\rm rad}$ follows immediately:

$$P = \sigma_{\rm T} c U_{\rm rad} \,,$$

with $U_{\rm rad} = S/c$ for a beam-like configuration. This is the classical picture of the IC loss rate: in the Thomson regime, the electron simply ***samples the ambient radiation field over an effective area $\sigma_{\rm T}$ and converts that intercepted flux into scattered photons***.

Finally, it is often convenient to quantify how likely it is for a photon to be Thomson scattered as it traverses a medium of free electrons. The corresponding ***Thomson optical depth***, which is the integrated scattering probability along a path, is

$$\tau_e = \int n_e \, \sigma_{\rm T} \, ds \,,$$

where n_e is the electron number density. Note that, from the photon's perspective, this is the "inverse process": the photon is the incoming particle and the electron acts as the scattering target.

Compton scattering formula. We now turn to a fully relativistic, quantum description of photon–electron scattering. This will naturally lead us to Compton's formula and, ultimately, to the Klein–Nishina cross-section that governs the high-energy regime.

The Compton scattering process, involving the interaction of photons with electrons, is most cleanly described in the language of four-vectors. We impose energy–momentum conservation in the scattering process:

$$K_i^\mu + P_i^\mu = K_f^\mu + P_f^\mu \,,$$

where $P_{i,f}^2 = m_e^2$ for the electron and $K_{i,f}^2 = 0$ for the photons (we are using units with $c = 1$ for the four-vectors).

Contracting the final electron four-momentum with itself, we obtain

$$P_f^\mu P_{f\mu} = (P_i + K_i - K_f)^\mu (P_i + K_i - K_f)_\mu \quad \Rightarrow \quad m_e^2 = m_e^2 + 2(P_i K_i - P_i K_f - K_i K_f)\,.$$

In the electron rest frame, we have $P_i = (m_e, \mathbf{0})$, and we choose the x-axis along the direction of the incoming photon. Then

$$K_i = \epsilon_i(1, 1, 0, 0) \quad \text{and} \quad K_f = \epsilon_f(1, \cos\theta, \sin\theta, 0)\,,$$

where $\epsilon_{i,f}$ are the initial and final photon energies in this frame, and θ is the scattering angle between the incoming and outgoing photon.

Substituting these expressions into the previous equation, we find

$$m_e^2 = m_e^2 + 2\left(m_e\epsilon_i - m_e\epsilon_f - \epsilon_i\epsilon_f + \epsilon_i\epsilon_f\cos\theta\right) \quad \Rightarrow \quad m_e(\epsilon_i - \epsilon_f) = \epsilon_i\epsilon_f(1 - \cos\theta)\,.$$

Solving for the final photon energy yields the ***Compton formula***:

$$\epsilon_f = \frac{\epsilon_i}{1 + \dfrac{\epsilon_i}{m_e c^2}(1 - \cos\theta)}\,. \tag{1.38}$$

This relation tells us how the photon energy changes as a function of its initial energy and the scattering angle θ.

It is useful to rewrite this as a fractional energy change:

$$\frac{\Delta\epsilon}{\epsilon} = \frac{\epsilon_f - \epsilon_i}{\epsilon_i} = -1 + \frac{1}{1 + \dfrac{\epsilon_i}{m_e c^2}(1 - \cos\theta)} \overset{\epsilon_i \ll m_e c^2}{\longrightarrow} -\frac{\epsilon_i}{m_e c^2}(1 - \cos\theta)\,.$$

This is the essence of *Compton scattering*: a photon collides with an electron and transfers some of its energy to the electron, emerging with a lower energy $\epsilon_f < \epsilon_i$. The key point is that, unless the photon energy in the electron rest frame is comparable to or larger than the electron rest mass, the fractional energy change remains small.

At this stage we can also refine our interpretation of the Thomson formula **??**. Previously we viewed $U_{\rm rad}$ as the energy density of the ***incoming*** radiation field. The Compton formula reminds us, however, that what really matters for the energy balance is the energy carried away by the ***scattered*** photons. For a given bin of incoming photons with energy ϵ_i, the number density is $n_\gamma(\epsilon_i)\,d\epsilon_i$, but after scattering each of those photons emerges with energy $\epsilon_f(\epsilon_i, \theta)$. The total energy density in the scattered field is therefore

$$U_{\rm rad} = \int n_\gamma(\epsilon_i)\,\epsilon_f(\epsilon_i, \theta)\,d\epsilon_i. \tag{1.39}$$

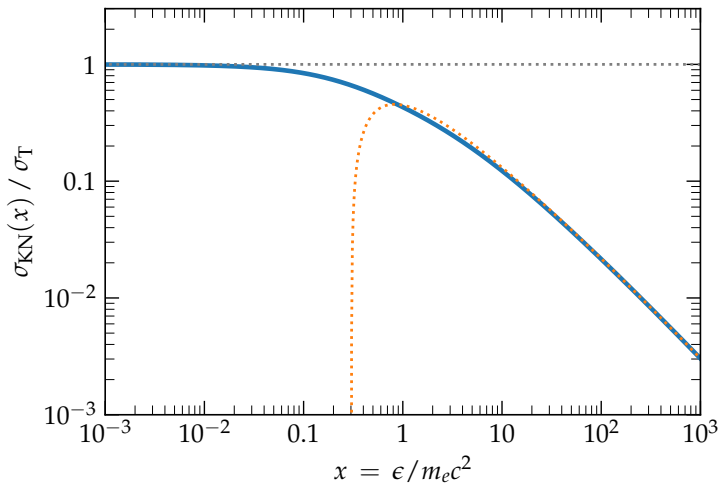

Figure 1.5: The Klein-Nishina cross section as a function of the adimensional photon energy x. At low ($x \ll 1$) energies, Thomson regime applies ($\sigma_{\rm KN}/\sigma_{\rm T} \simeq 1$). In KN regime $x \gg 1$, cross section is much reduced. The dashed line is the approximation at high energies as given in **??**.

In the Thomson limit one has $\epsilon_f \simeq \epsilon_i$ in the electron rest frame, so $U_{\rm rad}$ reduces to the familiar incident energy density. Writing the integrand with ϵ_f simply anticipates the more general situation: once we go beyond Thomson, the photon energy does change in the electron frame, and it is this ***final*** energy that determines how much energy is gained by the radiation field and lost by the electron.

Klein–Nishina regime. We can now clearly distinguish the *Thomson regime* from the *Compton (Klein–Nishina) regime*:

- For $\epsilon_i \ll m_e c^2$, the scattering is almost elastic: $\epsilon_i \simeq \epsilon_f$, and the classical Thomson description applies.
- As ϵ_i approaches or exceeds $m_e c^2$, the energy transfer becomes significant and the scattering becomes genuinely inelastic. In this regime, the full Klein–Nishina cross-section must be used.

The full Klein–Nishina (KN) cross-section, derived within Quantum Electrodynamics, can be written as

$$\sigma_{\rm KN} = \frac{3}{4}\sigma_{\rm T}\left[\frac{1+x}{x^3}\left(\frac{2x(1+x)}{1+2x} - \ln(1+2x)\right) + \frac{1}{2x}\ln(1+2x) - \frac{1+3x}{(1+2x)^2}\right] , \tag{1.40}$$

where

$$x \equiv \frac{\epsilon_i}{m_e c^2}$$

is the dimensionless photon energy in the electron rest frame.

It is reassuring that this expression reproduces the Thomson limit for soft photons. For $x \ll 1$,

$$\sigma(x) \simeq \sigma_{\rm T}\,(1 - 2x + \dots) , \tag{1.41}$$

so that $\sigma_{\rm KN} \to \sigma_{\rm T}$ as $x \to 0$. In the opposite, extreme KN limit ($x \gg 1$), the cross-section is strongly suppressed:

$$\sigma(x) \simeq \frac{3}{8}\sigma_{\rm T}\frac{1}{x}\left(\ln 2x + \frac{1}{2}\right) . \tag{1.42}$$

Therefore, the principal effect of entering the KN regime is a *reduction* of the scattering cross-section relative to the classical Thomson value as the photon energy increases in the electron rest frame. For inverse Compton scattering in astrophysics, this means that very energetic electrons scattering off comparatively energetic photons become less efficient radiators than a naive Thomson estimate would suggest.

Single-particle power radiated in IC scattering. We now want to compute the average power radiated by a *single* ultra-relativistic electron moving through an isotropic photon bath, in the Thomson regime. The final result will mirror the synchrotron power:

$$P_{\rm IC} = \frac{4}{3}\,\sigma_{\rm T}\,c\,\gamma^2\beta^2\,U_{\rm rad}\,,$$

but it is worth seeing carefully how each factor arises.

Step 1: Power in the electron rest frame. In the Thomson regime, i.e. when the photon energy in the electron rest frame satisfies

$$\epsilon_i' \ll m_e c^2\,,$$

scattering is almost elastic and the classical Thomson result for the scattered power applies. In the rest frame of the electron (primed quantities), the power scattered is simply

$$\frac{dE'}{dt'} = \sigma_{\rm T}\,c\,U'_{\rm rad}\,, \tag{1.43}$$

where $U'_{\rm rad}$ is the radiation energy density *as seen by the electron*. Our main task is to relate $U'_{\rm rad}$ to the radiation energy density $U_{\rm rad}$ measured in the LAB frame, and then interpret this power as an energy-loss rate for the electron in the LAB.

Strictly speaking, the Lorentz-invariant quantity is the energy loss per unit *proper time*, $dE/d\tau$, which is the time component of the 4-force. In the instantaneous rest frame of the electron we have $t' = \tau$, so $dE'/dt' = dE/d\tau$ and for our purposes we take

$$\frac{dE}{dt} = \frac{dE'}{dt'} = \sigma_{\rm T}\,c\,U'_{\rm rad} \tag{1.44}$$

as the working relation. The non-trivial part is therefore to compute $U'_{\rm rad}$.

Step 2: Transforming the radiation field to the electron frame. In the electron rest frame, the radiation field is described by (1.39):

$$U'_{\rm rad} = \int n'_\gamma(\epsilon'_i)\,\epsilon'_f(\epsilon'_i,\theta)\,d\epsilon'_i\,, \tag{1.45}$$

where n'_γ is the photon number density in the electron frame, ϵ'_i the incident photon energy, and ϵ'_f the scattered photon energy.

In the *Thomson* limit, in the electron rest frame the scattering is quasi-elastic:

$$\epsilon'_f \simeq \epsilon'_i \,,$$

so we can approximate

$$U'_{\rm rad} \simeq \int n'_\gamma(\epsilon'_i)\,\epsilon'_i\,d\epsilon'_i \,. \tag{1.46}$$

To connect n'_γ to n_γ, we use the Lorentz invariance of the phase-space distribution function. The occupation number

$$f(\mathbf{x},\mathbf{p}) = \frac{dN}{d^3\mathbf{x}\,d^3\mathbf{p}}$$

is a scalar: $f(\mathbf{x},\mathbf{p}) = f'(\mathbf{x}',\mathbf{p}')$. For photons, $|\mathbf{p}| = \epsilon/c$ and in an isotropic field we can write

$$n_\gamma(\epsilon)\,d\epsilon = f\,d^3\mathbf{p}\,.$$

Since f is invariant, $n_\gamma(\epsilon)\,d\epsilon$ must transform in the same way as $d^3\mathbf{p}$. One can show that this implies

$$\frac{n_\gamma(\epsilon)\,d\epsilon}{\epsilon} = \frac{n'_\gamma(\epsilon')\,d\epsilon'}{\epsilon'}\,, \tag{1.47}$$

i.e. n/ϵ is invariant under Lorentz transformations.

[add a formal derivation of this?]

Next we use the transformation law for photon energy. For a photon of LAB-frame energy ϵ_i propagating at angle θ with respect to the electron velocity β, the energy in the electron rest frame is

$$\epsilon'_i = \gamma\,\epsilon_i\,(1-\beta\cos\theta)\,, \tag{1.48}$$

where $\gamma = (1-\beta^2)^{-1/2}$ as usual. Combining (1.46)–(1.48), we can write $U'_{\rm rad}$ in terms of LAB-frame quantities.

Step 3: Expressing $U'_{\rm rad}$ in terms of $U_{\rm rad}$. Starting from (1.46), we use (1.47) to replace $n'_\gamma(\epsilon'_i)\,d\epsilon'_i$:

$$n'_\gamma(\epsilon'_i)\,d\epsilon'_i = n_\gamma(\epsilon_i)\,d\epsilon_i\,\frac{\epsilon'_i}{\epsilon_i}\,.$$

Thus

$$U'_{\rm rad} \simeq \int n'_\gamma(\epsilon'_i)\,\epsilon'_i\,d\epsilon'_i = \int \epsilon'_i\left[n_\gamma(\epsilon_i)\,d\epsilon_i\,\frac{\epsilon'_i}{\epsilon_i}\right] = \int \epsilon'^2_i\,\frac{n_\gamma(\epsilon_i)}{\epsilon_i}\,d\epsilon_i\,. \tag{1.49}$$

Using (1.48), we have

$$\epsilon'_i = \gamma\,\epsilon_i\,(1-\beta\cos\theta) \quad\Rightarrow\quad \epsilon'^2_i = \gamma^2\,\epsilon_i^2\,(1-\beta\cos\theta)^2\,.$$

Therefore

$$U'_{\rm rad} = \int \epsilon_i^2\, \gamma^2 (1 - \beta\cos\theta)^2\, \frac{n_\gamma(\epsilon_i)}{\epsilon_i}\, d\epsilon_i\,. \tag{1.50}$$

At this point we use the fact that the *incident* radiation field is isotropic in the LAB. This means that the angular dependence can be averaged separately from the energy dependence. Denoting $\mu = \cos\theta$, we compute

$$\frac{1}{2}\int_{-1}^{1} (1-\beta\mu)^2\, d\mu = \frac{1}{2}\int_{-1}^{1} (1 - 2\beta\mu + \beta^2\mu^2)\, d\mu\,.$$

The three terms give

$$\frac{1}{2}\int_{-1}^{1} d\mu = 1, \quad \frac{1}{2}\int_{-1}^{1} (-2\beta\mu)\, d\mu = 0, \quad \frac{1}{2}\int_{-1}^{1} \beta^2\mu^2\, d\mu = \beta^2\frac{1}{3}\,,$$

so that

$$\frac{1}{2}\int_{-1}^{1} (1-\beta\cos\theta)^2\, d\cos\theta = 1 + \frac{\beta^2}{3}\,. \tag{1.51}$$

Using this average in (1.50), and recognizing that the remaining energy integral is just $U_{\rm rad}$, we obtain

$$U'_{\rm rad} = \gamma^2 \left(1 + \frac{\beta^2}{3}\right) U_{\rm rad}\,. \tag{1.52}$$

Physically, this reflects the fact that, in its rest frame, the electron sees the originally isotropic photon bath ***boosted and anisotropic***, with more energetic photons coming from the forward direction (head-on collisions), which enhances the effective energy density.

Step 4: The IC power and its synchrotron twin. Plugging this result into (1.44), the angle-averaged Compton-scattered power (in the LAB frame) is

$$\frac{dE}{dt} = \sigma_{\rm T}\, c\, U'_{\rm rad} = \sigma_{\rm T}\, c\, \gamma^2 \left(1 + \frac{\beta^2}{3}\right) U_{\rm rad}\,. \tag{1.53}$$

However, this is still not quite the ***net*** power lost by the electron. Part of this power corresponds to the ***scattered*** radiation that would have existed even if the photon energies had not changed (i.e. if scattering were strictly elastic in the LAB). The actual energy lost by the electron equals the increase in the photon energy flux:

$$\frac{dE_e}{dt} = (\text{power in final photon field}) - (\text{power in initial photon field})\,.$$

The power carried by the incident photons through the effective cross-section $\sigma_{\rm T}$ is simply $P_{\rm in} = \sigma_{\rm T}\, c\, U_{\rm rad}$. The power in the scattered photons is $P_{\rm out} = \sigma_{\rm T} c\, U'_{\rm rad}$. Hence

$$\frac{dE_e}{dt} = \sigma_{\rm T} c\, U'_{\rm rad} - \sigma_{\rm T} c\, U_{\rm rad}\,. \tag{1.54}$$

Using $U'_{\rm rad} = \gamma^2 \left(1 + \frac{\beta^2}{3}\right) U_{\rm rad}$, we find

$$P_{\rm IC} \equiv -\frac{dE_e}{dt} = \sigma_{\rm T} c \left[\gamma^2 \left(1 + \frac{\beta^2}{3}\right) - 1\right] U_{\rm rad}$$
$$= \sigma_{\rm T} c \left(\gamma^2 + \frac{\gamma^2\beta^2}{3} - 1\right) U_{\rm rad} \,.$$

Using $\gamma^2 - 1 = \gamma^2\beta^2$, this simplifies to

$$P_{\rm IC} = \sigma_{\rm T} c \left(\gamma^2\beta^2 + \frac{\gamma^2\beta^2}{3}\right) U_{\rm rad} = \frac{4}{3}\,\sigma_{\rm T} c\,\beta^2\gamma^2\,U_{\rm rad} \,. \tag{1.55}$$

This is the ***net inverse-Compton power gained by the radiation field and lost by the electron***.

It is now very transparent why IC and synchrotron losses so often appear side by side. The total synchrotron power of a single relativistic electron in a magnetic field B was obtained in **??**. The analogy is obvious: in synchrotron, the electron interacts with a *magnetic* energy density $U_{\rm B}$; in inverse Compton, it interacts with a *photon* energy density $U_{\rm rad}$. Their ratio is simply

$$\frac{P_{\rm IC}}{P_{\rm s}} = \frac{U_{\rm rad}}{U_{\rm B}} \,,$$

provided absorption is negligible and we remain in the Thomson regime (no KN corrections). This is extremely useful in practice: once you know the magnetic field and the radiation background, you immediately know which process dominates the cooling of high-energy electrons.

Note also that both synchrotron and inverse-Compton powers scale as γ^2, so they have the same impact on the shape of the electron spectrum; their competition only changes the *timescale* via the ratio $U_{\rm rad}/U_{\rm B}$.

Average photon energy gain in the Thomson regime. A natural question at this stage is: what is the *average* energy of the up-scattered photons?

The number of photons scattered per unit time by one electron is of order

$$\frac{dN_s}{dt} \simeq \sigma_{\rm T}\, c\, n_{\rm ph} \,, \tag{1.56}$$

where $n_{\rm ph}$ is the photon number density. If we denote the average initial photon energy by

$$\langle \epsilon_i \rangle = \frac{\int \epsilon_i\, n_\gamma(\epsilon_i)\, d\epsilon_i}{\int n_\gamma(\epsilon_i)\, d\epsilon_i} \,,$$

we can write $U_{\rm rad} = n_{\rm ph}\,\langle\epsilon_i\rangle$ and therefore

$$\frac{dN_s}{dt} \simeq \frac{\sigma_{\rm T} c\, U_{\rm rad}}{\langle\epsilon_i\rangle}\,. \tag{1.57}$$

The total IC power is the product of the number of scattered photons per unit time and their average final energy:

$$P_{\rm IC} \simeq \langle\epsilon_f\rangle \frac{dN_s}{dt}\,.$$

Combining with the expression for $P_{\rm IC}$ derived in **??**, we obtain

$$\langle\epsilon_f\rangle = \frac{P_{\rm IC}}{dN_s/dt} = \frac{\frac{4}{3}\sigma_{\rm T} c\,\gamma^2\beta^2\,U_{\rm rad}}{\frac{\sigma_{\rm T} c\,U_{\rm rad}}{\langle\epsilon_i\rangle}} = \frac{4}{3}\,\gamma^2\beta^2\,\langle\epsilon_i\rangle\,. \tag{1.58}$$

For ultra-relativistic electrons ($\beta \simeq 1$),

$$\langle\epsilon_f\rangle \simeq \frac{4}{3}\,\gamma^2\,\langle\epsilon_i\rangle\,. \tag{1.59}$$

This is the classic result: ***in the Thomson regime, an ultra-relativistic electron boosts the photon energy on average by a factor*** $\sim \gamma^2$. This scaling will be essential when we compute IC spectra from a given electron distribution.

Beyond Thomson — KN corrections. If the photon energy in the electron rest frame is not negligible compared to $m_e c^2$, the scattering becomes inelastic even in that frame, and the Thomson approximation breaks down. A systematic expansion of the full Klein–Nishina cross-section (for an isotropic incident photon distribution) yields, for the electron energy-loss rate,

$$-\frac{dE_e}{dt} = P_{\rm IC} = \frac{4}{3}\gamma^2\beta^2\sigma_{\rm T} c U_{\rm rad}\left[1 - \frac{63}{10}\frac{\gamma}{m_e c^2}\frac{\langle\epsilon_i^2\rangle}{\langle\epsilon_i\rangle} + \ldots\right], \tag{1.60}$$

where

$$\langle\epsilon_i\rangle = \frac{\int \epsilon_i\, n_\gamma(\epsilon_i)\, d\epsilon_i}{\int n_\gamma(\epsilon_i)\, d\epsilon_i} \quad \text{and} \quad \langle\epsilon_i^2\rangle = \frac{\int \epsilon_i^2\, n_\gamma(\epsilon_i)\, d\epsilon_i}{\int n_\gamma(\epsilon_i)\, d\epsilon_i}\,.$$

This result (see Blumenthal & Gould 1970) shows explicitly that, once we leave the Thomson regime, the details of the *photon spectrum* become important: the loss rate depends not only on the total energy density $U_{\rm rad}$, but also on higher moments such as $\langle\epsilon_i^2\rangle$.

Physically, the KN regime reduces the effective cross-section for high-energy photons in the electron rest frame, thereby suppressing both the IC power and the average energy boost compared to the simple Thomson scaling. In the deep KN limit, the scattered photon energy in the electron rest frame saturates at $\epsilon_f' \sim O(m_e c^2)$, so that in the LAB

frame the characteristic scattered energy scales as $\epsilon_f \sim \gamma\, m_e c^2$, largely independent of the seed photon energy. In realistic astrophysical environments (e.g. hot radiation fields or very high-energy electrons), this KN suppression strongly reshapes both the IC cooling rate and the emergent photon spectrum.

It is useful to make explicit *when* the KN suppression sets in. The relevant dimensionless parameter is

$$x \equiv \frac{\epsilon_i'}{m_e c^2},$$

where ϵ_i' is the incident photon energy in the electron rest frame. Using the Lorentz transformation, $\epsilon_i' = \gamma\, \epsilon_i\, (1 - \beta \cos\theta)$, with ϵ_i the photon energy in the LAB and θ the angle between the photon and electron momenta. For the most effective (approximately head-on) scatterings, $(1-\beta\cos\theta) \sim O(1)$, so the condition $x \gtrsim 1$ can be written schematically as

$$\gamma\, \epsilon_i \sim m_e c^2.$$

In terms of the electron energy $E_e \simeq \gamma m_e c^2$, this translates into

$$E_e \sim \frac{(m_e c^2)^2}{\epsilon_i}. \tag{1.61}$$

Above this characteristic energy, IC scattering on photons of energy ϵ_i progressively enters the KN regime and the Thomson expression $P_{\rm IC} \propto \gamma^2$ ceases to apply.

Numerically, one finds

$$E_e^{\rm KN} \sim 260\ {\rm GeV} \left(\frac{\epsilon_i}{1\ {\rm eV}}\right)^{-1}, \tag{1.62}$$

so electrons with $E_e \gtrsim$ few $\times\, 10^2$ GeV already experience KN suppression when scattering optical/UV photons, while the corresponding threshold for CMB photons ($\epsilon_i \sim 10^{-3}$ eV) lies at $E_e \sim 10^5$–10^6 GeV.

1.6 Inverse-Compton emission by an electron population.

We can now repeat essentially the same argument for inverse-Compton (IC) scattering in the Thomson regime. This makes the deep symmetry between synchrotron and IC very explicit.

We again assume a power-law electron distribution as in **??**, but now the electrons radiate by scattering a background photon field. For clarity, let us start with a ***monochromatic*** and ***isotropic*** photon bath of frequency ν_0 and energy density $U_{\rm rad}$, and assume Thomson scattering throughout:

$$\epsilon_i' \ll m_e c^2 \quad \text{for all relevant } \gamma\text{'s}.$$

In this regime, the angle-averaged single-electron IC power is given by **??** and the characteristic scattered frequency is

$$\nu_{\rm IC}(\gamma) \simeq \frac{4}{3}\,\gamma^2\,\nu_0,$$

corresponding to the average photon energy gain $\langle \epsilon_f \rangle \simeq \frac{4}{3}\gamma^2 \epsilon_i$ derived earlier.

As for synchrotron, we now approximate the single-electron IC spectrum by a delta function at its characteristic frequency:

$$P_\nu^{\rm IC}(\gamma) \;\simeq\; \langle P_{\rm IC}(\gamma)\rangle\;\delta\big(\nu-\nu_{\rm IC}(\gamma)\big).$$

The IC emissivity is then

$$j_\nu^{\rm IC} = \int n(\gamma)\,P_\nu^{\rm IC}(\gamma)\,d\gamma = \int n_0\,\gamma^{-p}\,\langle P_{\rm IC}(\gamma)\rangle\,\delta\big(\nu-\nu_{\rm IC}(\gamma)\big)\,d\gamma.$$

We define

$$\nu_{\rm IC}(\gamma) \equiv C_{\rm IC}\,\gamma^2, \qquad C_{\rm IC} \equiv \frac{4}{3}\,\nu_0,$$

so that

$$\delta\big(\nu-\nu_{\rm IC}(\gamma)\big) = \frac{\delta\big(\gamma-\gamma_\nu\big)}{\left|\frac{d\nu_{\rm IC}}{d\gamma}\right|_{\gamma_\nu}}, \qquad \gamma_\nu = \sqrt{\frac{\nu}{C_{\rm IC}}}.$$

Proceeding as before, we obtain

$$j_\nu^{\rm IC} = n_0\,\frac{\langle P_{\rm IC}(\gamma_\nu)\rangle\,\gamma_\nu^{-p}}{\left|\dfrac{d\nu_{\rm IC}}{d\gamma}\right|_{\gamma_\nu}} = n_0\,\frac{\frac{4}{3}c\sigma_{\rm T}U_{\rm rad}\,\gamma_\nu^{2-p}}{2\,C_{\rm IC}\,\gamma_\nu} \propto U_{\rm rad}\,\nu_0^{-\frac{p+1}{2}}\,\nu^{-\frac{p-1}{2}}\,. \tag{1.63}$$

Thus the IC emissivity ***in the Thomson regime*** has the same frequency dependence as synchrotron:

$$j_\nu^{\rm IC} \;\propto\; n_0\,U_{\rm rad}\,\nu^{-\frac{p-1}{2}} \tag{1.64}$$

up to a factor depending smoothly on p and on the seed photon frequency ν_0. Comparing with the synchrotron result in **??**, the parallel is striking.

In words: in the Thomson regime and for a narrow seed photon distribution, a power-law in electrons with index p produces a synchrotron and an IC spectrum with the *same* spectral index $\alpha = (p-1)/2$. The relative normalization is set by the ratio $U_{\rm rad}/U_B$, in agreement with the single-electron power ratio

$$\frac{P_{\rm IC}}{P_{\rm s}} = \frac{U_{\rm rad}}{U_B}.$$

For broader seed photon spectra (e.g. a blackbody field), the IC emissivity is a convolution of the electron and photon distributions. As long as we stay in the Thomson regime and the photon spectrum does not vary too rapidly around the characteristic seed frequency for each γ, the IC spectrum still tends to inherit the $\nu^{-(p-1)/2}$ scaling over a wide frequency band, with additional curvature reflecting the seed field.

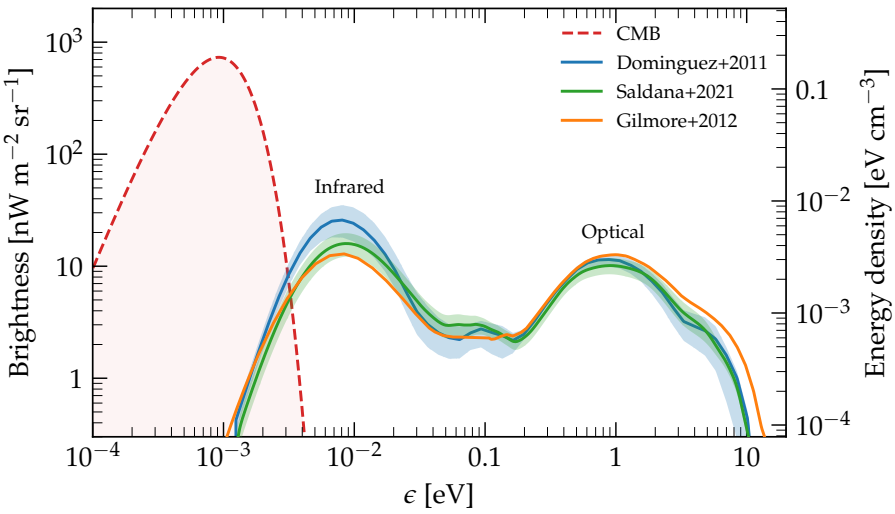

*Figure 1.6: Photon field energy density of the CMB and the extragalactic background light (EBL) as a function of photon energy. For the EBL we show three recent models from the literature [**?**, **?**, **?**].*

1.7 Pair production and gamma-ray absorption

High-energy γ rays emitted by distant sources (AGN, GRBs, star-forming galaxies) do not travel through a vacuum. Along their way, they encounter photons of the diffuse extragalactic radiation fields: the cosmic microwave background (CMB) and the extragalactic background light (EBL) from integrated starlight and dust emission (see Fig. 1.6).

When a γ-ray of energy E_γ interacts with a background photon of energy ϵ, it can produce an e^+e^- pair,

$$\gamma + \gamma \;\rightarrow\; e^+ + e^-,$$

provided that the center-of-mass (CoM) energy exceeds the rest mass of the pair. This process leads to ***attenuation*** of the primary γ-ray flux, and defines an effective ***γ-ray horizon***.

Threshold condition and target photon energies. The pair-production kinematics are controlled by the Lorentz-invariant squared CoM energy,

$$s = (P_a + P_b)^2 = m_a^2 + m_b^2 + 2(E_a E_b - \mathbf{p}_a \cdot \mathbf{p}_b).$$

For two photons ($m_a = m_b = 0$, $|\mathbf{p}| = E/c$) with energies E_γ and ϵ and angle θ between their momenta,

$$s = 2E_\gamma \epsilon (1 - \cos\theta),$$

in units where $c = 1$. The threshold for producing an e^+e^- pair is when the CoM energy is just enough to create two electrons at rest in the CoM frame,

$$s_{\rm th} = (2m_e c^2)^2 = 4m_e^2 c^4.$$

Thus the threshold condition is

$$2E_\gamma \epsilon (1 - \cos\theta) \;\geq\; 4m_e^2 c^4. \tag{1.65}$$

For a head-on collision ($\theta = \pi$, $1 - \cos\theta = 2$),

$$4E_\gamma \epsilon \;\geq\; 4m_e^2 c^4 \quad\Rightarrow\quad E_\gamma \epsilon \;\geq\; m_e^2 c^4,$$

or

$$E_\gamma \;\gtrsim\; \frac{(m_e c^2)^2}{\epsilon}. \tag{1.66}$$

As very useful rule-of-thumb, high-energy γ-rays mainly interact with target photons whose energy satisfies

$$E_\gamma(\text{TeV})\, \epsilon(\text{eV}) \;\gtrsim\; 0.26.$$

For example:

- A 1 TeV photon ($E_\gamma = 10^{12}$ eV) interacts at threshold with photons of $\epsilon_{\rm th} \simeq 0.26$ eV, i.e. near-infrared photons.
- A 10 TeV photon primarily interacts with optical photons ($\epsilon_{\rm th} \sim$ few eV).
- A 100 GeV photon interacts most efficiently with UV photons ($\epsilon_{\rm th} \sim O(10\text{ eV})$).

Center-of-mass velocity and cross-section. To describe the pair-production cross-section, it is convenient to introduce the velocity β^* of the produced electron (or positron) in the CoM frame. In that frame, the electron and positron have equal and opposite momenta, and each has energy

$$E_e^* = \gamma^* m_e c^2,$$

with

$$\gamma^* = \frac{1}{\sqrt{1 - \beta^{*2}}}.$$

The total CoM energy is

$$\sqrt{s} = 2E_e^* = 2\gamma^* m_e c^2 \quad\Rightarrow\quad \gamma^* = \frac{\sqrt{s}}{2m_e c^2}.$$

From this,

$$\beta^* = \sqrt{1 - \frac{1}{\gamma^{*2}}} = \sqrt{1 - \frac{4m_e^2 c^4}{s}} = \sqrt{1 - \frac{2m_e^2 c^4}{E_\gamma \epsilon (1 - \cos\theta)}}.$$

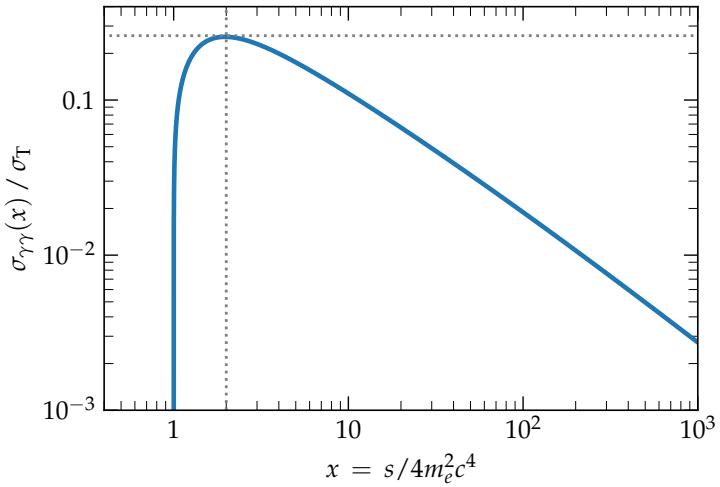

Figure 1.7: .

The exact $\gamma\gamma \to e^+e^-$ cross-section in terms of β^* is derived by QED [add citation]:

$$\sigma_{\gamma\gamma}(\beta^*) = \frac{3}{16}\sigma_{\mathrm{T}}\,(1-\beta^{*2})\left[2\beta^*(\beta^{*2}-2) + (3-\beta^{*4})\ln\left(\frac{1+\beta^*}{1-\beta^*}\right)\right], \tag{1.67}$$

where σ_{T} is the Thomson cross-section. The threshold corresponds to $\beta^* \to 0$, while the ultra-relativistic limit of the pair corresponds to $\beta^* \to 1$.

A few key features of $\sigma_{\gamma\gamma}$:

- *Near threshold* ($\beta^* \ll 1$), the cross-section rises steeply from zero.
- It reaches a maximum value of order

  $$\sigma_{\gamma\gamma}^{\max} \simeq 0.25\,\sigma_{\mathrm{T}}\ ,$$

  for CoM energies a few times above threshold ($s \sim$ few $\times\, 4m_e^2c^4$).
- In the *high-energy limit* ($\beta^* \to 1$, $s \gg 4m_e^2c^4$), the cross-section falls off roughly as $1/s$, i.e. as the inverse of the product $E_\gamma\epsilon$. A standard asymptotic expression is

  $$\sigma_{\gamma\gamma}(\beta^*) \simeq \frac{3}{8}\frac{\sigma_{\mathrm{T}}}{\gamma^{*2}}\left[\ln\left(4\gamma^{*2}\right) - 1\right] \propto \frac{1}{\gamma^{*2}} \simeq \frac{1}{E_\gamma\epsilon(1-\cos\theta)}. \tag{1.68}$$

Physically, this means that γ rays can in principle interact with all target photons above the threshold, but the interaction is ***most efficient*** when the product $E_\gamma\epsilon$ is only a few times the threshold value. At much higher energies, the cross-section shrinks, and the Universe becomes more transparent again.

Optical depth and the γ-ray horizon. The cumulative effect of $\gamma\gamma$ interactions ***along the line of sight*** is encoded in the optical depth $\tau_{\gamma\gamma}(E_\gamma)$, defined as the integral over path

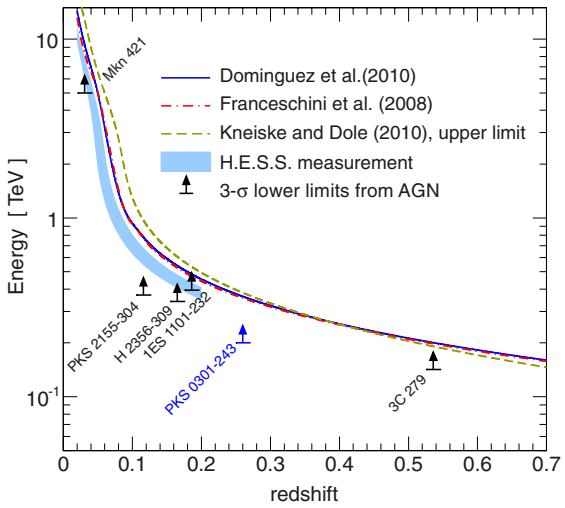

*Figure 1.8: γ-ray horizon for different EBL models. Some lower limits from AGN spectra measurements are shown [**?**].*

length, angles, and target photon energies:

$$\tau_{\gamma\gamma}(E_\gamma) = \int_0^R dx \int_{4\pi} d\Omega\,(1-\cos\theta) \int_{\epsilon_{\rm th}}^{\infty} d\epsilon\, n_\gamma(\epsilon,\Omega,x)\,\sigma_{\gamma\gamma}(E_\gamma,\epsilon,\cos\theta). \tag{1.69}$$

Here:

- x is the distance along the line of sight (or, in cosmological applications, a redshift coordinate),
- $n_\gamma(\epsilon,\Omega,x)$ is the differential number density of background photons at position x with energy ϵ and direction Ω,
- $(1-\cos\theta)$ accounts for the angular dependence of the CoM energy,
- $\epsilon_{\rm th}$ is the local threshold energy from (1.65).

The observed flux is then attenuated as

$$F_{\rm obs}(E_\gamma) = F_{\rm int}(E_\gamma)\,\exp\big[-\tau_{\gamma\gamma}(E_\gamma)\big],$$

where $F_{\rm int}$ is the intrinsic source spectrum.

For extragalactic sources at redshift z, one typically defines the *γ-ray horizon* $E_{\gamma,\,\rm hor}(z)$ as the energy at which $\tau_{\gamma\gamma}(E_\gamma,z) = 1$. For $E_\gamma \gg E_{\gamma,\,\rm hor}(z)$ the flux is exponentially suppressed. Different EBL models predict different $\tau_{\gamma\gamma}(E_\gamma,z)$ curves; comparisons with AGN spectra yield constraints on the EBL, as illustrated in Fig. 1.8.

However, an order-of-magnitude $\gamma\gamma$ optical depth can be estimated for a photon from a source at cosmological distance using the simple approximation

$$\tau_{\gamma\gamma} \;\sim\; \sigma_{\gamma\gamma}\, n_\gamma\, L\,.$$

Assuming a TeV photon, the head-on threshold condition for pair production implies that the dominant target photons have energies

$$\epsilon_{\rm th} \simeq 1\ {\rm eV},$$

i.e. in the optical/near-IR band. Let us assume that the extragalactic background light (EBL) around $\epsilon \sim 1$ eV has a typical *energy density* (see Fig. **??**):

$$u_{\rm EBL} \sim 3\times10^{-3}\ {\rm eV\,cm^{-3}},$$

comparable to a few percent of the CMB energy density. The corresponding photon number density is then

$$n_\gamma \sim \frac{u_{\rm EBL}}{\epsilon_{\rm th}} \sim 3\times10^{-3}\ {\rm cm^{-3}}.$$

The pair-production cross-section $\sigma_{\gamma\gamma}(s)$ peaks at a value

$$\sigma_{\gamma\gamma}^{\rm max} \sim 0.25\,\sigma_{\rm T} \sim 1.7\times10^{-25}\ {\rm cm^2}.$$

Requiring $\tau_{\gamma\gamma} \sim 1$ gives a characteristic interaction length

$$L \sim \frac{1}{\sigma_{\gamma\gamma}\,n_\gamma} \sim \frac{1}{(1.7\times10^{-25}\ {\rm cm^2})\,(3\times10^{-3}\ {\rm cm^{-3}})} \sim 2\times10^{27}\ {\rm cm} \sim 0.6\ {\rm Gpc}.$$

Thus, up to factors of a few, an optical depth $\tau_{\gamma\gamma} \sim 1$ is expected on distance scales of order a gigaparsec. In a flat ΛCDM cosmology, this is the right ballpark for the proper distance to sources at $z \sim 1$, explaining why TeV γ rays from such redshifts are strongly attenuated by pair production on the EBL.

[add electromagnetic cascades]

A | Appendix

A.1 Motion of a Charged Particle in a Uniform Magnetic Field

We work in c.g.s. Gaussian units. A particle of charge q and rest mass m moves with velocity $\mathbf{v}$ in a constant magnetic field $\mathbf{B}$. We denote $\beta \equiv v/c$, $\gamma = (1-\beta^2)^{-1/2}$, and $\hat{\mathbf{b}} \equiv \mathbf{B}/B$ (the unit vector along the field).

The starting point is the Lorentz force,

$$\dot{\mathbf{p}} \equiv \frac{d}{dt}(\gamma m \mathbf{v}) = q\left(\mathbf{E} + \frac{\mathbf{v}}{c} \times \mathbf{B}\right).$$

Throughout this appendix we set $\mathbf{E} = 0$. This is a good idealization in many astrophysical plasmas: in the fluid rest frame the electric field vanishes because of the extremely high conductivity (ideal MHD).

A first and very useful observation is that a magnetic field does no work:

$$\frac{dE}{dt} = \mathbf{v}\cdot\dot{\mathbf{p}} = q\,\mathbf{v}\cdot\mathbf{E} = 0 \quad \Rightarrow \quad E = \gamma m c^2 = \text{const.}$$

Hence, both γ and the speed $|\mathbf{v}|$ are constant in time. The acceleration is therefore purely geometric: it can only *change the direction* of $\mathbf{v}$, not its magnitude.

With $\mathbf{E} = 0$ the equation $\gamma m\,\mathbf{a} = \frac{q}{c}\,\mathbf{v} \times \mathbf{B}$ immediately gives

$$\mathbf{v}\cdot\mathbf{a} = \frac{q}{\gamma m c}\,\mathbf{v}\cdot(\mathbf{v}\times\mathbf{B}) = 0,$$

so $\mathbf{a} \perp \mathbf{v}$: the acceleration is centripetal (curvature) rather than tangential (speed change).

To describe the motion, decompose the velocity into components parallel and perpendicular to $\mathbf{B}$,

$$\mathbf{v} = v_\parallel \hat{\mathbf{b}} + \mathbf{v}_\perp.$$

Projecting the Lorentz equation along $\mathbf{B}$ yields

$$\frac{d}{dt}(\gamma m v_\parallel) = \frac{q}{c}\,\mathbf{B}\cdot(\mathbf{v}\times\mathbf{B}) = 0 \quad \Rightarrow \quad p_\parallel = \gamma m v_\parallel = \text{const.}$$

Because $p = \gamma m v$ is also constant (the speed is fixed), the *perpendicular* component is constant as well:

$$p_\perp = \sqrt{p^2 - p_\parallel^2} = p\sqrt{1-\mu^2} = \text{const}, \qquad \mu \equiv \frac{p_\parallel}{p} = \cos\theta.$$

In other words, the *pitch angle* θ between the momentum and the field line is conserved.

In the plane orthogonal to $\mathbf{B}$ we have

$$\gamma m \frac{d\mathbf{v}_\perp}{dt} = \frac{q}{c}\,\mathbf{v}_\perp \times \mathbf{B}, \qquad \frac{dv_\parallel}{dt} = 0,$$

i.e. uniform circular motion plus uniform drift along $\mathbf{B}$. Choosing coordinates with $\mathbf{B} = B\,\hat{\mathbf{z}}$ and introducing an initial phase ϕ_0, an explicit solution is

$$\begin{aligned} v_x(t) &= -\,v_\perp \sin\!\big(\Omega_B t + \phi_0\big), & x(t) &= x_g + r_g \cos\!\big(\Omega_B t + \phi_0\big), \\ v_y(t) &= \;\; v_\perp \cos\!\big(\Omega_B t + \phi_0\big), & y(t) &= y_g + r_g \sin\!\big(\Omega_B t + \phi_0\big), \\ v_z(t) &= v_\parallel = \beta c\,\mu, & z(t) &= z_g + v_\parallel t, \end{aligned}$$

where (x_g, y_g, z_g) are the guiding–center coordinates, and $v_\perp = \Omega_B r_g$ ties the speed to the radius as in any circular motion. The path is a *helix* of fixed radius and constant pitch.

These results introduce two natural scales. The *gyro* (relativistic) angular frequency and the gyroradius are

Remark.

$$\Omega_B = \frac{qB}{\gamma mc} = \frac{\Omega_0}{\gamma}, \qquad r_g = \frac{v_\perp}{\Omega_B} = \frac{\gamma mc\, v_\perp}{qB} = \frac{p_\perp c}{qB}\,. \tag{A.1}$$

Here

$$\Omega_0 \equiv \frac{qB}{mc}$$

is the *cyclotron* (non-relativistic) angular frequency; dividing by 2π gives ordinary frequencies ν_0 and $\nu_B = \nu_0/\gamma$. The factor of γ has a clear interpretation: relativity *slows* the rotation as seen in the lab frame (time dilation), so the frequency drops by $1/\gamma$ while the radius grows by γ at fixed $v_\perp$.

Cosmic particles are often relativistic ($v_\perp \simeq c$), for which

$$r_g \simeq \frac{\gamma mc^2}{qB} \;\approx\; \frac{E}{qB}\,.$$

Remark. Magnetic rigidity. It is often convenient to define the *magnetic rigidity* $R \equiv pc/|q|$, so that

$$r_g = \frac{R}{B}\,.$$

For ultra-relativistic particles ($p \simeq E/c$) and charge number $Z = |q|/e$,

$$r_g \simeq 1.08\ \text{pc} \left(\frac{E}{\text{PeV}}\right)\left(\frac{Z\,B}{\mu\text{G}}\right)^{-1},$$

a handy back-of-the-envelope rule for Galactic and extragalactic settings.

For quick reference, Table A.1 recaps the symbols and their relativistic/non-relativistic forms, and Table A.2 provides order-of-magnitude scales relevant to cosmic-ray physics.

Quantity	**Non-relativistic**	**Relativistic**
Angular frequency	$\Omega_0 = \dfrac{qB}{mc}$	$\Omega_B = \dfrac{qB}{\gamma mc} = \dfrac{\Omega_0}{\gamma}$
Ordinary frequency	$\nu_0 = \dfrac{\Omega_0}{2\pi} = \dfrac{1}{2\pi}\dfrac{qB}{mc}$	$\nu_B = \dfrac{\Omega_B}{2\pi} = \dfrac{\nu_0}{\gamma}$
Gyroradius	$r_0 = \dfrac{mc\,v_\perp}{qB}$	$r_g = \dfrac{\gamma mc\,v_\perp}{qB} = \gamma r_0$

Table A.1: Notation used in these notes. Here $v_\perp$ is the speed perpendicular to $\mathbf{B}$; $p_\perp = \gamma m v_\perp$. For $v_\perp \simeq c$, $r_g \simeq \gamma mc^2/(qB)$.

Quantity	**Galactic CR**	**UHECR**
	$B \sim 1\ \mu\mathrm{G},\ E \sim 10\ \mathrm{GeV}$	$B \sim 1\ \mathrm{nG},\ E \sim 1\ \mathrm{EeV}$
Angular freq. Ω_B	$\sim 10^{-3}\ \mathrm{s}^{-1}$	$\sim 10^{-14}\ \mathrm{s}^{-1}$
Ordinary freq. ν_B	$\sim 10^{-4}\ \mathrm{Hz}$	$\sim 10^{-15}\ \mathrm{Hz}$
Gyroradius r_g	$\sim 3\times10^{13}\ \mathrm{cm}\ \approx\ 10^{-5}\ \mathrm{pc}$	$\sim 3\times10^{24}\ \mathrm{cm}\ \approx\ \mathrm{Mpc}$

Table A.2: Representative scales for a proton ($Z = 1$) with $v_\perp \simeq c$. For general Z, $r_g \propto 1/Z$ and $\Omega_B, \nu_B \propto Z$.